Chemical Engineering Journal 476 (2023) 146655

Contents lists available at ScienceDirect

Chemical Engineering Journal

journal homepage: www.elsevier.com/locate/cej

Continuous-flow titration of low iron doses to promote photo-Fenton and photo-Fenton-like processes at neutral pH

Carla Santos [a,b], Miguel Herraiz-Carboné [c], Engracia Lacasa [c], Cristina Sáez [d], Rosa Montes [e], José Benito Quintana [e], Rosario Rodil [e], Ana I. Gomes [a,b,*], Vítor J.P. Vilar [a,b,*]

[a] Laboratory of Separation and Reaction Engineering-Laboratory of Catalysis and Materials (LSRE-LCM), Chemical Engineering Department, Faculty of Engineering University of Porto, Rua Dr. Roberto Frias, 4200-465 Porto, Portugal

[b] Associate Laboratory in Chemical Engineering (ALiCE), Faculty of Engineering, University of Porto, Rua Dr. Roberto Frias, 4200-465 Porto, Portugal

[c] Department of Chemical Engineering, Higher Technical School of Industrial Engineering, University of Castilla-La Mancha, Edificio Infante Don Juan Manuel, Campus Universitario s/n, 02071 Albacete, Spain

[d] Department of Chemical Engineering, Faculty of Chemical Sciences and Technologies, University of Castilla-La Mancha, Edificio Enrique Costa Novella, Campus Universitario s/n, 13005 Ciudad Real, Spain

[e] Department of Analytical Chemistry, Nutrition and Food Sciences, Institute of Research on Chemical and Biological Analysis (IAQBUS), Universidade de Santiago de Compostela, Constantino Candeira S/N, 15782 Santiago de Compostela, Spain

ARTICLE INFO

Keywords:
Contaminants of emerging concern
Iron radial addition
Phosphate precipitation
Tubular membrane photoreactor
Urban wastewater treatment

ABSTRACT

Photo-Fenton (PF) is a promising process for degrading a wide range of contaminants of emerging concern (CECs) present in urban wastewater (UWW) after secondary treatment, mitigating their spread in aquatic systems. However, the near-neutral pH of UWW poses a challenge to PF performance. In this research, a tubular membrane photoreactor, designed for continuous "titration" of Fe^{2+}, is explored to promote the PF process for the tertiary treatment of UWW. The application of persulfate (PF-like) as an alternative oxidant and the impact of phosphate (PO_4^{3-}) content in UWW were also assessed. Process efficiency was evaluated in continuous mode, applying low residence times (RT: 6.1, 36.6, and 73.2 s) and low Fe^{2+} doses (1, 2, and 5 mg L^{-1}), for the oxidation of 19 CECs (each spiked at 10 μg/L), in demineralized water (DW) and secondary-treated UWW. Despite the persistence of certain short-chain perfluoroalkyl substances (PFAS) and saccharine across all conditions tested, the PF-like process exhibited superior performance when compared with PF, attaining higher removals for most target CECs, especially for melamine. In UWW, for an RT = 73.2 s, [Fe^{2+}] = 5 mg L^{-1}, and [oxidant] = 1.2 mM, PF process removed 7 CECs > 60 % and PF-like 10 CECs > 60 %. Moreover, higher residual concentrations of Fe^{2+} and lower precipitation of PO_4^{3-} were observed for PF-like treatments, evidencing its advantages for tertiary treatment. These results emphasize the importance of photoreactor design to achieve efficient PF/PF-like at neutral pH, avoiding the use of chelating agents while managing iron concentrations compatible with UWW discharge or reuse limits.

1. Introduction

The limited performance of wastewater treatment plants (WWTPs) in removing contaminants of emerging concern (CECs) such as personal care products, pharmaceutical and endocrine disrupting compounds or drugs, among others, has led to alarming levels of these substances in natural waters [1,2]. The accumulation of CECs, even at low concentrations, can have detrimental effects on animal communities by interfering with hormonal functions, disrupting the trophic chain through bioaccumulation and biomagnification, and potentially causing adverse effects on human health (imbalance in hormonal and reproductive systems or metabolic, neurological and immunological disorders) [3,4]. In this context, the development of advanced and efficient technologies capable of removing these contaminants from wastewater matrices is paramount to prevent their accumulation in natural waters.

Among several advanced oxidation processes (AOPs), the photo-Fenton (PF) process has emerged as one of the most attractive methods for the removal of CECs from urban wastewaters (UWW) [5,6].

* Corresponding authors at: Laboratory of Separation and Reaction Engineering-Laboratory of Catalysis and Materials (LSRE-LCM), Chemical Engineering Department, Faculty of Engineering University of Porto, Rua Dr. Roberto Frias, 4200-465 Porto, Portugal.

E-mail addresses: ana.isabelgomes@fe.up.pt (A.I. Gomes), vilar@fe.up.pt (V.J.P. Vilar).

https://doi.org/10.1016/j.cej.2023.146655
Received 28 June 2023; Received in revised form 25 September 2023; Accepted 11 October 2023
Available online 17 October 2023

This process is characterized by the massive generation of hydroxyl ($HO^{\cdot}$) radicals through a chain reaction between a catalyst (ferrous ion: Fe^{2+}) and an oxidant (hydrogen peroxide: H_2O_2) and by the photolysis (UV light) of ferric complexes enabling Fe^{2+} regeneration. Persulfate ($S_2O_8^{2-}$) can also be applied as an oxidant in place of H_2O_2. In this case, a PF-like process occurs in which the reaction between $S_2O_8^{2-}$ and Fe^{2+} generates sulfate radicals ($SO_4^{\cdot-}$) with high oxidation potential (E^0 = 2.60 V) able to oxidize a wide range of organic contaminants [7,8]. The unique characteristics of $SO_4^{\cdot-}$ radicals, such as being strong electron acceptors, allow alternative reaction pathways to those with $HO^{\cdot}$ radicals [9]. Moreover, $SO_4^{\cdot-}$ presents a longer lifetime and greater selectivity than $HO^{\cdot}$, and the technologies based on $SO_4^{\cdot-}$ radical show very satisfactory efficiencies with respect to the reduction and mineralization of environmental contaminants [10].

It is well known that the ideal pH for the PF process is 2.8 since keeping the pH close to 3 ensures the dissolution of iron and the predominance of the most photoactive ferric complexes [11]. Nevertheless, UWW after secondary treatment typically has a near-neutral pH, requiring acidification before PF treatment and a subsequent neutralization before discharge to the receiving environment, which incurs economic disadvantages and environmental drawbacks. Consequently, recent efforts have focused on operating the PF process at mild pH conditions to degrade CECs in UWW (Table 1). A widely studied approach involves the addition of chelating agents, macromolecules with carboxylic and/or amino groups (e.g., ethylenediaminetetraacetic acid, EDTA [12], ethylenediaminedisuccinic acid, EDDS [13,14,19] which promote the formation of photoactive iron complexes with improved solubility and photoactivity (Table 1 for details on the cited research). However, the addition of high concentrations of the chelating agent is normally required, undesirably increasing the treatment costs and the organic carbon content in the effluent under treatment and, consequently, competing with the pollutants for oxidative species [6,22]. Another approach (Table 1) involves the controlled addition of low concentrations of iron salts, constant [21] or intermittent dosage [15,17], during the reaction period to facilitate the continuous generation of oxidizing species during phototreatment.

Photoreactor design is also critical for achieving a highly efficient PF process at neutral pH conditions. Compound parabolic reactors (CPCs) and raceway pond reactors (RPRs) have been widely applied for this purpose (Table 1). Although both have the advantage of using sunlight as a source of radiation, CPCs are recognized as a technology with high manufacturing and amortization costs, while RPRs are economically attractive but less efficient in capturing photons [6]. Furthermore, in some cases, high amounts of iron catalyst are added, leading to high final concentrations of iron (e.g. works by Carra et al. [15] and Starling et al. [17], see Table 1), which jeopardize compliance with the legal limits for direct discharge into the aquatic system or water reuse for irrigation. This can be overcome by resorting to the continuous addition of low iron dose along the reactor length, as demonstrated by Díaz-Angulo et al. [21], by employing a tubular membrane photoreactor. Beyond the advantage of being operated in continuous mode, this system allows a uniform distribution of the catalyst (Fe^{2+}) along the entire reactor length due to its radial addition into the annular reaction zone (ARZ) through the pores of the membrane. Also, the acidic character of the Fe^{2+} solution permeating through the membrane minimizes iron precipitation in the liquid thin film around the membrane shell-side and promotes the regeneration of ferric (Fe^{3+}) to ferrous (Fe^{2+}) ions under UV light.

With this background, this work focuses on the application of the PF ($UVC/H_2O_2/Fe^{2+}$) and PF-like ($UVC/S_2O_8^{2-}/Fe^{2+}$) processes at neutral pH for the tertiary treatment of UWW applying the tubular membrane photoreactor. Process efficiency was evaluated for the removal of a

Table 1
Studies reported in the literature for different strategies to operate the photo-Fenton process at neutral pH for the removal of CECs in UWW.

Strategy	Target CECs	Reactor	Operational conditions	Main results	Reference
Addition of complexing agents	22 CECs naturally present (ranging from 16 to 66379 ng/L, for cotinine and caffeine, respectively)	Compound parabolic collector (pilot-scale)	Batch mode; pH = 6.5; $[Fe^{3+}] = 5$ mg L^{-1}; [EDDS] = 0.2 mM; $[H_2O_2] = 50$ mg L^{-1}; Solar radiation (30 W m^{-2})	95 % removal after 63 min	[14]
	Levofloxacin (2 mg L^{-1})	Compound parabolic collector (lab-scale)	Batch mode; pH = 5.0; $[Fe^{3+}] = 2.0$ mg L^{-1} + oxalate 1:3 M ratio; $[H_2O_2] = 20$ mg L^{-1}; Solar simulator (41.6 W m^{-2})	71 % removal after 60 min	[20]
	Carbamazepine, Crotamiton, Ibuprofen (462.6, 394.6 and 101.1 ng/L, respectively)	Glass vessel (lab-scale)	Batch mode; pH = 7.6; $[Fe^{3+}] = 9.9$ mg L^{-1} + NTA 1:1 M ratio; $[H_2O_2] = 154$ mg L^{-1}; UVA radiation (4.05 mW cm^{-2})	92 % removal after 120 min	[18]
	Sulfamethoxazole and Imidacloprid (50 μg/L)	Raceway pond (pilot-scale)	Batch mode; pH = 6–7; $[Fe^{3+}] = 5.6$ mg L^{-1} + EDDS or NTA 1:1 M ratio; $[H_2O_2] = 30$ mg L^{-1}; Solar radiation (35 ± 2 W m^{-2})	>60 % removal after 60 min and 5 cm depth	[16]
	Propranolol (1.9 μM)	Tubular photoreactor (lab-scale)	Batch mode; pH = 7.6–8; $[Fe^{2+}] = 0.18$ mM + DTPA or EDTA 1:1 M ratio; $[H_2O_2] = 4.41$ mM; UVA radiation (8 LEDs, 2.66×10^{-7} Einstein L^{-1} s^{-1})	Fe^{2+}:DTPA – 94 % removal after 120 min Fe^{2+}:EDTA – 100 % removal after 15 min	[12]
	17 CECs naturally present (ranging from 15 to 3926 ng/L, for diazepam and 4-FAA, respectively)	Raceway pond (pilot-scale)	Continuous mode; pH = 6.1–7.5; $[Fe^{3+}] = 0.1$ mM + EDDS 1:1 M ratio; $[H_2O_2] = 0.88$ mM; prior removal of carbonate species; Solar radiation	≈60 % removal after 20 min and 5 cm depth	[13]
	Sulfamethoxazole (50 μg/L)	Raceway pond (pilot-scale)	Batch mode; pH = 6.5–7.5; $[Fe^{3+}] = 5.6$ mg L^{-1} + EDDS 1:1 M ratio; $[H_2O_2] = 30$ mg L^{-1}; Solar radiation (average 26 ± 4 W m^{-2})	≈80 % removal after 15 min and 5 cm depth	[19]
Intermittent or continuous addition of small doses of iron salts	Pesticides (Vydate, Metmur, Couraze, Perfekthion and Scala) (10 mg L^{-1} of DOC for each)	Compound parabolic collector (pilot-scale)	Batch mode; pH = 7; Addition of 20 mg Fe^{2+} L^{-1} at t = 0 and 5 min, then 10 mg Fe^{2+} L^{-1} at t = 15, 25 and 35 min, $[Fe^{2+}]_{total} = 70$ mg L^{-1} and $[Fe^{2+}]_{average} = 13.5$ mg L^{-1}; $[H_2O_2] = 650$ mg L^{-1}; Solar radiation (30 W m^{-2})	49 % removal after 60 min	[15]
	Caffeine, Carbendazim, and Losartan (100 μg L^{-1} each)	Raceway pond (pilot-scale)	Batch mode; pH = 7; Addition of Fe^{2+} at t = 0, 5, 10, 15 and 20 min, $[Fe^{2+}]_{total} = 55$ mg L^{-1}; $[S_2O_8^{2-}] = 288$ mg L^{-1}; Solar radiation (average 30 W m^{-2})	55 % removal after 60 min	[17]
	Amoxicillin (2 mg L^{-1})	Tubular membrane photoreactor	Continuous mode; pH = 7.4; Continuous addition of a iron stock solution ($[Fe^{2+}]_{stock} = 1700$ mg L^{-1}), targeting a $[Fe^{2+}]_{reaction}$ of 5 mg L^{-1}; $[H_2O_2] = 40$ mg L^{-1}; UVC radiation (useful 1.7 W)	46 % removal after 4.6 s	[21]

mixture of 19 CECs representing diverse chemical groups (pharmaceutical compounds, sweeteners, a fire retardant, an herbicide, an insect repellent, and several short chain perfluoroalkyl substances (PFAS)), with different chemical behaviors and reactivities towards oxidation processes. These 19 target CECs were selected under the NOR-WATER project due to their occurrence and persistence in WWTP effluents and river basins of Northern Portugal and Galicia [23,24]. The influence of iron dosage, oxidant type and concentration, retention time (RT), and water matrix (demineralized water (DW) *vs* secondary-treated UWW) on the degradation of the 19 target CECs was evaluated. Additionally, the impact of a pre-treatment to precipitate phosphates (PO_4^{3-}) present in the secondary-treated UWW was evaluated.

2. Materials and methods

2.1. Chemicals and secondary-treated UWW

The selected target CECs (Table 2) were supplied by Sigma-Aldrich, TCI, AlfaAesar, and ACROS Organics (Purity > 95 %). Hydrogen peroxide (H_2O_2) was supplied by Fisher Chemical and sodium persulfate ($Na_2S_2O_8$) by Merck. Iron (II) sulfate heptahydrate ($FeSO_4{\cdot}7H_2O$) was used as received from Panreac. Ammonium metavanadate (NH_4VO_3, Merck) was used for the determination of H_2O_2, and potassium iodide (KI, Merck) and sodium bicarbonate ($NaHCO_3$, Merck) were employed for the quantification of $S_2O_8^{2-}$. Acetic acid, ascorbic acid, ammonium acetate (Fisher Chemical), and 1,10-phenanthroline monohydrate (Panreac) were used to determine Fe^{2+} and total dissolved iron (TDI). Sulfuric acid (Fisher Chemical), oxalic acid (VWR), and sodium sulfite (VWR) were used to adjust the pH, clean the experimental setup, and stop oxidation reactions at the end of treatment, respectively.

Feed solutions were prepared using DW (Panice® reverse osmosis system) or secondary-treated UWW, spiked with 10 μg/L of each target CEC. The UWW was collected downstream from the second clarifier of a municipal WWTP located in the North of Portugal and stored at 4 °C until its use. The native content of the 19 target CECs in the UWW is found in Table 2. The main physicochemical characteristics of the secondary-treated UWW, as received and after pre-treatment to precipitate PO_4^{3-} content up to ~50 %, ~100 %, and ~100 % followed by filtration, are summarized in Table 3.

Table 3
Physicochemical characteristics of the secondary-treated UWW as received and after pre-treatment to precipitate PO_4^{3-} (~50 %, ~100 %, and ~100 % followed by filtration).

Parameters (units)	UWW	UWW after precipitation of PO_4^{3-}		
		~50 %	~100 %	~100 % + filtration
Color		Pale/Yellow		
Odor		Not detected		
pH	7.4	7.3	7.2	7.4
Temperature (°C)	20.7	20.7	20.7	20.7
Dissolved Inorganic Carbon (mg L^{-1})	77.2	76.2	73.1	63.3
Dissolved Organic Carbon (mg L^{-1})	23.3	20.3	18.1	15.5
Absorbance UV254 (cm^{-1})	0.3	0.7	0.7	0.2
SUVA (L mg^{-1} m^{-1})	2.3	5.7	6.4	2.0
Chemical Oxygen Demand (mg L^{-1})	39.5	40.3	62.6	35.7
Volatile Suspended Solids (mg L^{-1})	2.3	7.0	10.7	1.0
Total Suspended Solids (mg L^{-1})	4.0	44.3	67.7	6.3
Total dissolved iron (mg L^{-1})	0.3	0.2	0.2	0.1
Phosphates (PO_4^{3-}) (mg L^{-1})	16.8	10.7	0.5	1.0
Sulfates (SO_4^{2-}) (mg L^{-1})	67.5	89.1	108.4	108.7
Nitrites (NO_2^-) (mg L^{-1})	6.3	6.8	6.6	7.2
Chlorides (Cl^-) (mg L^{-1})	161.3	160.9	159.9	161.2
Nitrates (NO_3^-) (mg L^{-1})	3.1	2.4	2.3	1.9
Bromides (Br^-) (mg L^{-1})	<0.06	<0.06	<0.06	<0.06
Sodium (Na^+) (mg L^{-1})	132.6	134.1	132.3	137.6
Ammonium (NH_4^+) (mg L^{-1})	77.6	73.0	72.9	74.7
Potassium (K^+) (mg L^{-1})	31.0	33.2	30.5	31.9
Magnesium (Mg^{2+}) (mg L^{-1})	8.7	8.3	8.1	8.3
Calcium (Ca^{2+}) (mg L^{-1})	34.4	33.4	31.2	31.4

Table 2
Identification of the 19 target CECs, respective limits of quantification, native content in the secondary-treated UWW, and rate constants for reaction with $HO^{\cdot}$ and $SO_4^{\cdot-}$.

Category	Pollutant	Acronym	Chemical composition	LQ_{DW} [a] (μg/L)	LQ_{UWW} [a] (μg/L)	UWW (μg/L)	$k_{HO^{\cdot}}$ [b] (M^{-1} s^{-1})	$k_{SO_4^{\cdot-}}$ [b] (M^{-1} s^{-1})
Angiotensin II Receptor Blockers	Valsartan	VSTN	$C_{24}H_{29}N_5O_3$	0.28	0.44	<0.44	1×10^{10}	Unknown
	Irbesartan	ISTN	$C_{25}H_{28}N_6O$	0.05	0.08	1.6	1×10^{10}	Unknown
	Losartan	LSTN	$C_{22}H_{22}ClKN_6O$	0.15	0.26	0.4	Unknown	Unknown
Sweeteners	Acesulfame	ACK	$C_4H_4KNO_4S$	0.5	0.68	0.7	4.6×10^9	$<2 \times 10^7$
	Saccharin	SCH	$C_7H_5NO_3S$	1	1.1	<1.1	1.6×10^9	4.1×10^8
Beta-blocking agents	Atenolol	ATNL	$C_{14}H_{22}N_2O_3$	0.15	0.24	<0.24	8×10^9	5.1×10^9
	Bisoprolol	BSPL	$C_{18}H_{31}NO_4$	0.04	0.11	<0.11	Unknown	Unknown
Carbamazepine and Metabolites	Carbamazepine	CBZ	$C_{15}H_{12}N_2O$	0.02	0.03	0.9	8.8×10^9	2.6×10^9
	10.11 Carbamazepine-epoxide	CBZ-EPX	$C_{15}H_{12}N_2O_2$	0.02	0.02	5.5	Unknown	Unknown
Fire Retardants	Melamine	MLN	$C_3H_6N_6$	0.58	0.75	11.3	1×10^4	1×10^5
Herbicides	Diuron	DRN	$C_9H_{10}Cl_2N_2O$	0.07	0.07	0.1	6.6×10^9	2.8×10^8
Hormones	17β-Estradiol	E2	$C_{18}H_{24}O_2$	2.1	3.1	<3.1	5.1×10^9	1.2×10^9
	17α-Ethinylestradiol	EE2	$C_{20}H_{24}O_2$	1.5	2.3	<2.3	9.8×10^9	3×10^9
Insect Repellents	N.N-diethyl-*meta*-toluamide	DEET	$C_{12}H_{17}NO$	0.03	0.03	0.4	5×10^9	3×10^8
Anti-Inflammatory Drugs	Diclofenac	DCF	$C_{14}H_{10}Cl_2NNaO_2$	0.18	0.19	2.6	7.5×10^9	9.2×10^9
Short Chain Perfluoroalkyl Substances (PFAS)	Heptafluorobutyric acid	HFBA	$C_4HF_7O_2$	0.14	0.14	<0.14	Unknown	Unknown
	Potassium nonafluoro-1-butanesulfonate	PFBS	$C_4F_9KO_3S$	0.09	0.09	<0.09	Unknown	Unknown
	Perfluorooctanoic acid	PFOA	$C_8HF_{15}O_2$	0.02	0.02	<0.02	$< 1 \times 10^5$	2.6×10^5
	Trifluoromethanesulfonic acid	TFMS	CHF_3O_3S	1	1.2	<1.2	$< 1 \times 10^5$	Unknown

[a] Limit of quantification for demineralized water matrix (LQ_{DW}) and secondary-treated urban wastewater (LQ_{UWW}).
[b] Kinetic constants for the reaction with $HO^{\cdot}$ (k_{HO}) and with $SO_4^{\cdot-}$ ($k_{SO_4^{\cdot-}}$) were obtained from Stauter et al. [28], Bourgin et al. [36], Toth et al. [27], Ye et al. [26], Huber et al. [37], Lian et al. [30], Rao et al. [38], Maurino et al. [32], Mezyk et al. [35], Song et al. [31], Zhou et al. [29], Umar [33], Qian et al. [34], Ahmed et al. [25].

2.2. Experimental setup

The lab-scale tubular membrane photoreactor system used in this work is displayed in Fig. 1. The detailed description of this system can be found elsewhere [39]. In brief, the tubular membrane photoreactor consists of a tubular ceramic ultrafiltration membrane (γ-Al_2O_3 from Inopor GmbH, pore size = 10 nm, cut-off = 20 kDa, porosity = 30 – 55 %, $Ø_{outer}$ = 20.3 mm, $Ø_{inner}$ = 15.5 mm, length = 200 mm), concentrically inserted inside a quartz tube ($Ø_{outer}$ = 32.0 mm, $Ø_{inner}$ = 28.0 mm, length = 200 mm), sealed by polypropylene flanges. Four lamps (Puritec HNS 6 W G5, from Philips) located around the quartz tube (annular reaction zone (ARZ): illuminated length of 174 mm and pathlength of 3.85 mm) were used as UVC light sources (λ_{max} = 254 nm). UVC radiation was chosen because it reacts with both catalyst and oxidants (ε_{254,H_2O_2} = 19.6 M^{-1} cm^{-1} and $\varepsilon_{254,S_2O_8^{2-}}$ = 21.1 M^{-1} cm^{-1}) and it is also already applied in disinfection systems installed in WWTPs. The lamps were surrounded by a cylindrical stainless steel cap and provided a photon flux of 0.8 ± 0.2 W (determined by actinometry with ferrioxalate, according to Hatchard and Parker [40]. The effluent was fed with a gear pump (Ismatec BVP-Z) to the ARZ, flowing in a helix trajectory around the membrane shell-side. For experiments with partial recirculation of the effluent, a second-gear pump (Ismatec BVP-Z) was coupled to the system. Oxidants (H_2O_2 or $S_2O_8^{2-}$) were dosed with a peristaltic pump (Gilson Minipuls 2) and added to the effluent at the reactor inlet. The Fe^{2+} stock solution was injected into the membrane via a syringe pump (Nexus 6000 from Chemyx Inc.) and forced to permeate through the pores to reach the membrane shell-side.

2.3. Experimental procedure

The experiments using the tubular membrane photoreactor were carried out in continuous mode. DW or secondary-treated UWW fortified with 10 μg/L of each CEC ($pH_{DW+CECs}$ = 6.5 ± 0.2; $pH_{UWW+CECs}$ = 7.8 ± 0.2) was transferred into the feed tank of the system and pumped through the ARZ. Simultaneously, the dosing of the catalyst (Fe^{2+} stock solution of 500 or 1700 mg L^{-1}, pH = 2.0 ± 0.1) and of the oxidant (equimolar doses of H_2O_2 or $S_2O_8^{2-}$) was initiated, fixing their flow rates to obtain the intended concentrations in the ARZ (1, 2 or 5 mg Fe^{2+} L^{-1} and 0.3, 0.6 or 1.2 mM of the oxidant), and the four lamps were switched on. Catalyst and oxidant dosages were selected based on our previous study [21]. The maximum amount of iron for the experiments in UWW also considered the limit of 5 mg L^{-1} indicated by the Food and Agriculture Organization (FAO) of the United Nations for long-term use of water reuse for irrigation purposes [41]. When the steady state is reached (Fig. 2), a minimum of three samples were taken to determine the final concentration of CECs, iron species (Fe^{2+} and Fe^{3+}), residual oxidant, and final pH. To stop the oxidation process, a solution of Na_2SO_3 was immediately added to the samples in a 5:1 M ratio with respect to the oxidant. At the end of each experiment, the reactor was thoroughly washed with an oxalic acid solution recirculated in the ARZ and then with distilled water.

For the experiments with DW, the feed flow rate (Q_F) was set at 30 L h^{-1}, corresponding to a residence time (RT) of 6.1 s. For comparison purposes, the removal of CECs was also evaluated in acidified DW (pH = 3.1 ± 0.1). For the experiments with UWW, partial recirculation of the

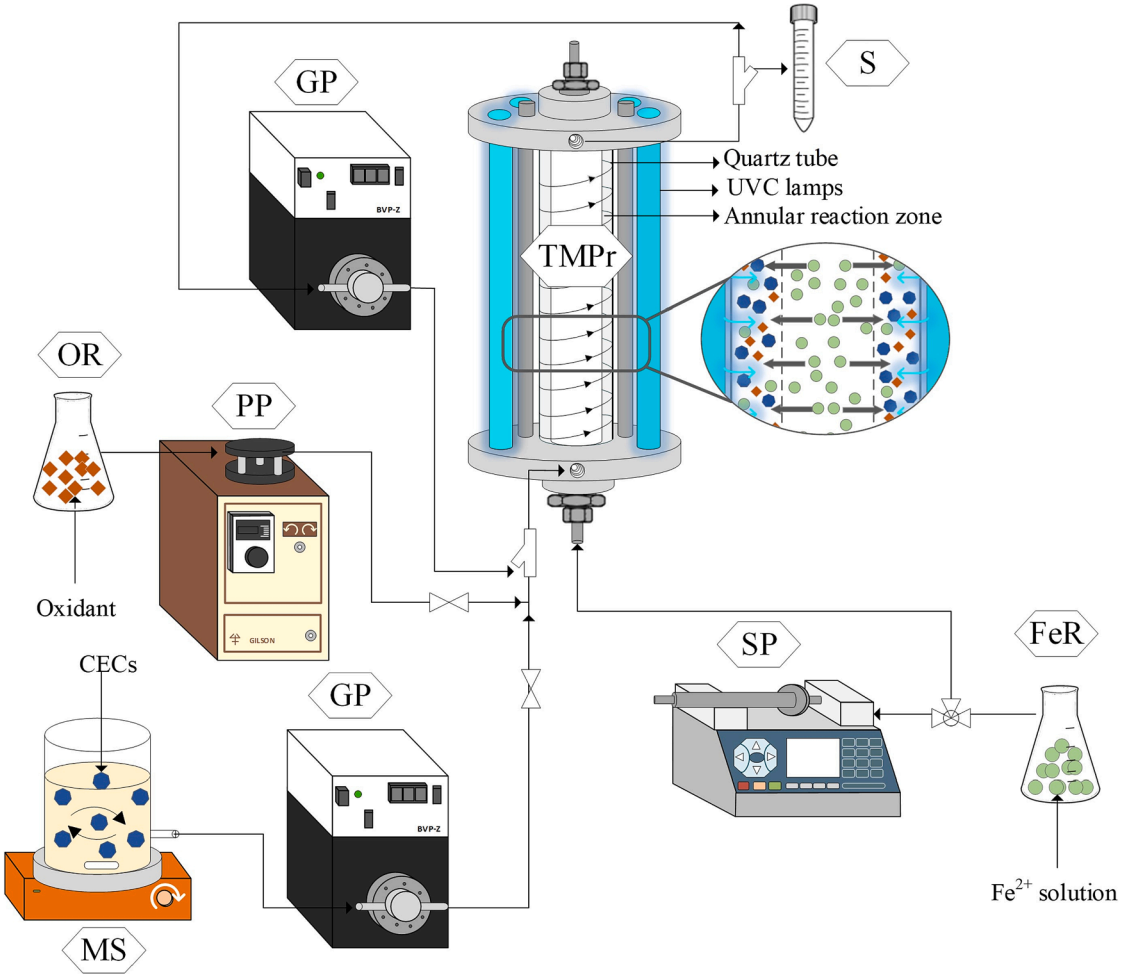

Fig. 1. Simplified schematics of the experimental setup. Legend: FeR – Iron stock solution reservoir; GP – Gear pump; MS – Magnetic stirrer; OR – Oxidant reservoir; PP – Peristaltic pump; S – Sampling; SP – Syringe pump; TMPr – Tubular membrane photoreactor.

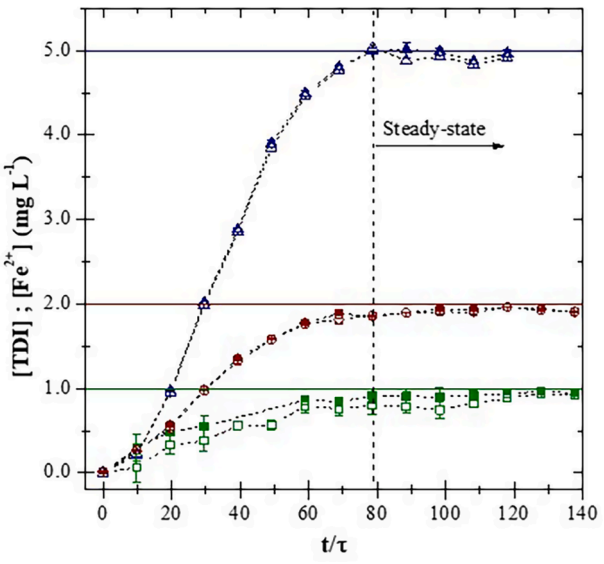

Fig. 2. Total dissolved iron (TDI, filled symbols) and Fe^{2+} (empty symbols) concentration profiles at the reactor outlet in the absence of radiation for intended concentrations in the ARZ of 1 mg L^{-1} (squares), 2 mg L^{-1} (circles), and 5 mg L^{-1} (triangles).

effluent was also carried out. In this case, the feed and recirculation flows were adjusted to keep the flow rate in the ARZ at 30 L h^{-1} (Q_F/Q_R = 30/0; 5/25 and 2.5/27.5 L h^{-1}) while increasing the RT (from 6.1 to 36.6 and 73.2 s, respectively). To evaluate the effect of PO_4^{3-} content on phototreatment, experiments were also carried out with UWW in which a pre-treatment to precipitate PO_4^{3-} was made. $FeSO_4{\cdot}7H_2O$ was added to the UWW considering the stoichiometric molar ratio of 1:1 (iron: phosphate) to precipitate c.a. 50 and 100 % of the PO_4^{3-} present in this matrix (Table 3). The solutions were vigorously mixed and settled for 4 h. Additionally, post-filtration was carried out (particle retention >1.2 μm) to decrease the concentration of TSS in the effluent with ~100 % PO_4^{3-} precipitation (Table 3). Table 4 summarizes the conditions employed in each experiment. To verify the reproducibility of the degradation results, replicates were carried out on independent days for the test conditions of exp. #3 and #8, for DW matrix, and exp. #15 and #21, for UWW (Fig. 1-SM, in the Supplementary file).

2.4. Analytical determinations

H_2O_2 and $S_2O_8^{2-}$ concentrations were determined spectrophotometrically using a UV–Vis VWR UV-6300 Double Beam analyzer at wavelengths of 450 and 352 nm, respectively, according to the methods proposed by Nogueira et al. [42] and Liang et al. [43]. Similarly, Fe^{2+} and total dissolved iron (TDI) concentrations were determined spectrophotometrically at 510 nm, following the method with 1,10-phenanthroline, according to ISO 6332 [44]. Analytical procedures for the main physicochemical characterization of the UWW were carried out according to recognized international standards whose methods are described in Table SM-1 of the Supplementary file.

Quantification of CECs was performed by ultra-performance liquid chromatography with an Acquity UPLC® coupled to a XEVO TQD® triple quadrupole mass spectrometer equipped with an electrospray interface (ESI) from Waters (Milford, MA, USA) following the methodology published in Presumido et al. [45]. The limits of quantification (LOQs) for each target CEC in the evaluated DW and UWW are shown in Table 2.

3. Results and discussion

3.1. Performance of the PF and PF-like processes in CECs removal using demineralized water

3.1.1. PF process: Effect of catalyst and oxidant doses

The efficiency of CECs oxidation was first analyzed for the UVC/H_2O_2 process (Eq. (1)), i.e., in the absence of the catalyst (Exp. #1). The results showed very slight degradation of CBZ, the artificial sweetener ACK, and the herbicide DRN (between 14 % and 17 %) and moderate removal for the metabolite CBZ-EPX (~30 %) and the anti-inflammatory drug DCF (~40 %) (Fig. 3a). For the remaining CECs, the variations in the measured concentrations were below 10 %, thus considered as negligible, taking into account method uncertainty.

$$H_2O_2 + h\nu \rightarrow 2HO^{\cdot} \ (\lambda = 254\ nm,\ \varepsilon = 19.6\ M^{-1}cm^{-1},\ \varphi = 0.50\ mol\ Einstein^{-1}) \quad (1)$$

By introducing the catalyst (Exp. #2 and #3, with 1 and 2 mg Fe^{2+} L^{-1}, respectively), additional $HO^{\cdot}$ radicals are generated (Eqs. (2) and (3)) and, consequently, a greater number of CECs presented slight removals (Fig. 3a). In addition to CBZ, DRN and ACK, the insect repellent DEET, β-blocking agents (ATNL and BSPL), and angiotensin II receptor blockers (VSTN and LSTN) also recorded removals between 12 % and 25 %. Once again, CBZ-EPX and DCF stand out with a higher level of removal (about 30 % and 70 %, respectively). In general, doubling the catalyst dose did not improve the removal of the target CECs, which may be explained by (i) a decreased light transmission due to greater iron precipitation and/or (ii) limitation of the oxidant dose. Considering the latter, the oxidant dose was doubled (Exp. #4: UVC + 0.6 mM H_2O_2 + 2 mg Fe^{2+} L^{-1}) and the CECs removal was improved (Fig. 3a). Note that under neutral pH conditions, dissolved iron precipitates as ferric hydroxide, so Eq. (3) is not expected to take place. However, in this system, acidic pH values can occur in the vicinity of the membrane shell-side, since the catalyst stock solution that is being permeated through the membrane pores has a pH of 2. This feature will contribute, to some extent, to minimize iron precipitation at local points close to the membrane and allow the regeneration of Fe^{3+} to Fe^{2+} under UV light as described by Eq. (3).

$$Fe^{2+} + H_2O_2 \rightarrow Fe^{3+} + HO^{-} + HO^{\cdot} \quad (2)$$

$$[Fe(OH)]^{2+} + h\nu \rightarrow Fe^{2+} + HO^{\cdot} \quad (3)$$

3.1.2. PF process: Effect of catalyst stock solution and initial pH

The influence of the [Fe^{2+}] stock solution on the removal of CECs in DW was also evaluated (Exp #5: $[Fe^{2+}]_{stock}$ = 500 mg L^{-1}). The results showed a marked improvement in the removal of the target CECs when compared with Exp. #3, where a more concentrated catalyst stock solution was applied (Fig. 3b). This is justified by the acidification of DW in Exp. #5 (pH_{final} = 4.4 *vs* pH_{final} = 5.5 of Exp. #3, Table 4), contributing to keep dissolved the iron species involved in the PF reactions. This acidification occurs because of the increase in the permeation flux of the acidic catalyst stock solution (from 0.6 to 2.0 mL min^{-1}) required to maintain $[Fe^{2+}]_{ARZ}$ at 2 mg Fe^{2+} L^{-1}.

The performance of the PF process at optimum pH conditions was also tested by a preliminary acidification of the DW at pH 3.1 (Exp. #6). As expected, the results showed enhanced treatment performance, obtaining the oxidation of a higher number of compounds (15 of the 19 CECs) and higher removal percentages (Fig. 3b). Specifically, degradations in the range of 60 to 80 % for 5 CECs (ATNL, CBZ, CBZ-EPX, DEET and LSTN) and > 80 % for 7 CECs (BSLP, DCF, DRN, E2, EE2, ISTN, and VSTN) were obtained. In turn, the artificial sweetener SCH was only removed ~30 %, and no significant degradation (<10 %) of MLN was observed. Similarly, the contaminants HFBA, PFBS, and TFMS, which belong to the group of short-chain perfluoroalkyl substances (PFAS,

Table 4
Experimental conditions for CECs removal experiments.

#	Matrix	Oxidant	[Oxidant] $_{ARZ}$ (mM)[a]	[Fe^{2+}] $_{stock}$ (mg L^{-1})	[Fe^{2+}] $_{ARZ}$ (mg L^{-1})	RT (s)	PO_4^{3-} precipitation (%)	UWW filtration	pH		[Fe^{2+}] $_{residual}$ (mg L^{-1})	TDI (mg L^{-1})	[Oxidant] $_{residual}$ (mM)	[PO_4^{3-}] $_{residual}$ (mg L^{-1})
									Initial	Final				
1	Demineralized Water (DW)	H_2O_2	0.3	n.a.	n.a.	6.1	n.a.	n.a.	6.4	6.5	n.a.	n.a.	0.3	n.a.
2			0.3	1700	1		n.a.	n.a.	6.8	6.2	< 0.2	0.28 (±0.01)	0.3	n.a.
3			0.3	1700	2		n.a.	n.a.	6.8	5.5	< 0.2	0.25 (±0.04)	0.2	n.a.
4			0.6	1700	2		n.a.	n.a.	6.7	5.6	< 0.2	<0.2	0.5	n.a.
5			0.3	500	2		n.a.	n.a.	6.6	4.4	< 0.2	0.26 (±0.06)	0.2	n.a.
6			0.3	500	2		n.a.	n.a.	3.1	3.1	< 0.2	2.06 (±0.03)	0.2	n.a.
7		$S_2O_8^{2-}$	0.3	n.a.	n.a.	6.1	n.a.	n.a.	6.3	6.1	n.a.	n.a.	0.1	n.a.
8			0.3	1700	2		n.a.	n.a.	6.4	4.0	< 0.2	0.49 (±0.02)	0.2	n.a.
9			0.6	1700	2		n.a.	n.a.	6.4	4.0	< 0.2	0.32 (±0.01)	0.5	n.a.
10	Urban Wastewater (UWW)	H_2O_2	1.2	1700	5	6.1	No	No	7.7	7.5	0.33 (±0.02)	0.72 (±0.03)	1.0	9.9
11			1.2	1700	5	36.6	No	No	7.7	7.6	0.26 (±0.02)	0.47 (±0.02)	0.9	8.1
12			1.2	1700	5	73.2	No	No	7.7	7.8	< 0.2	0.24 (±0.02)	0.8	7.3
13			1.2	1700	5	73.2	≈50	No	7.7	7.9	< 0.2	< 0.2	1.0	8.3
14			1.2	1700	5	73.2	≈100	No	8.1	8.0	< 0.2	< 0.2	0.8	< 0.5
15			1.2	1700	5	73.2	≈100	Yes	7.6	7.7	< 0.2	< 0.2	1.0	< 0.5
16		$S_2O_8^{2-}$	1.2	1700	5	6.1	No	No	7.7	7.5	0.86 (±0.03)	2.27 (±0.05)	1.0	13.2
17			1.2	1700	5	36.6	No	No	7.7	7.5	0.48 (±0.05)	1.44 (±0.02)	0.9	13.0
18			1.2	1700	5	73.2	No	No	7.8	7.4	< 0.2	0.49 (±0.02)	0.9	8.1
19			1.2	1700	5	73.2	≈50	No	7.7	7.6	< 0.2	< 0.2	1.1	8.2
20			1.2	1700	5	73.2	≈100	No	8.1	7.7	< 0.2	< 0.2	1.1	0.7
21			1.2	1700	5	73.2	≈100	Yes	7.8	7.5	< 0.2	0.48 (±0.01)	1.1	0.6

n.a. – not applicable.
[a] Oxidant concentrations of 0.3, 0.6 and 1.2 mM are equivalent to 10, 20 and 40 mg L^{-1} of H_2O_2 or 56, 113 and 226 mg L^{-1} of $S_2O_8^{2-}$.

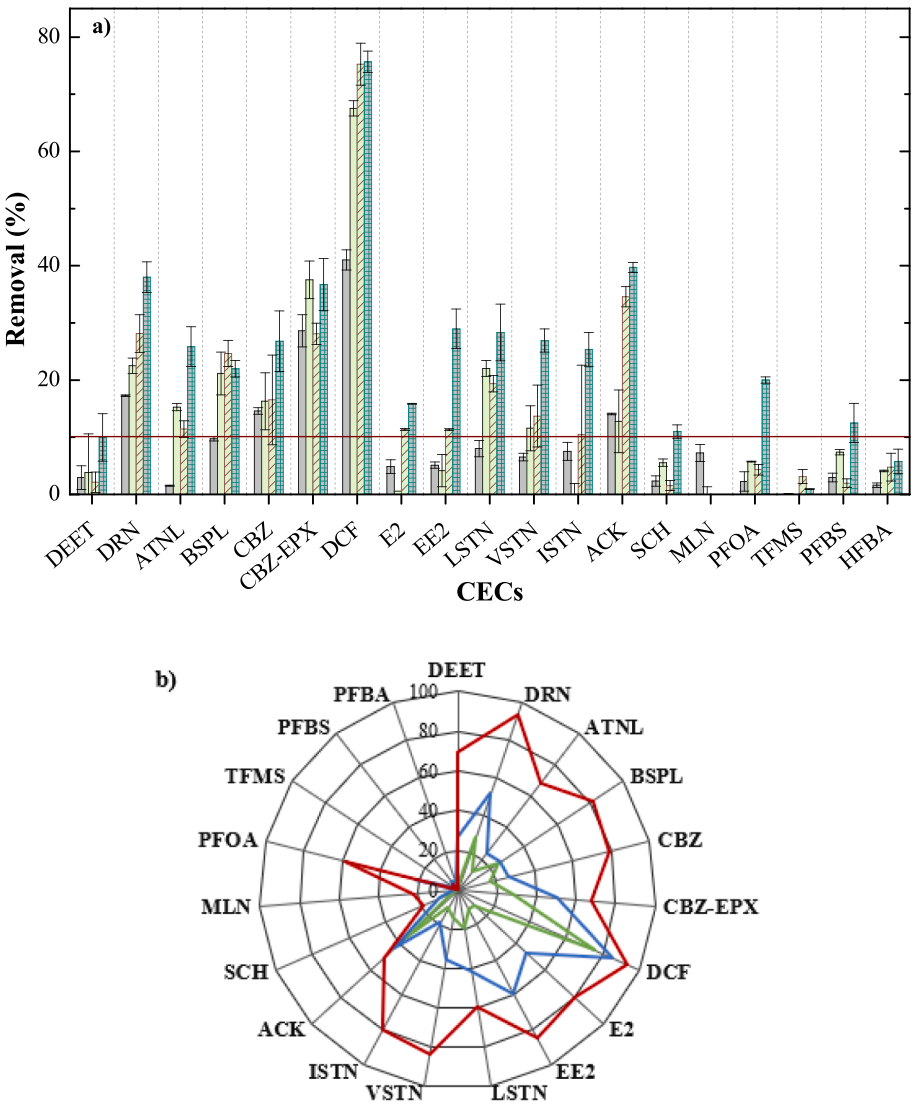

Fig. 3. Removal efficiencies (%) for the 19 target CECs spiked in DW a) in the absence of the catalyst (Exp. #1) and under different catalyst and oxidant concentrations (Exp. #2; Exp. #3; and Exp. #4) and b) comparison between PF experiments carried out with near-neutral initial pH applying different $[Fe^{2+}]_{stock}$ (Exp. #3 and Exp. #5) and with initial pH of 3.1 (Exp. #6). The operational conditions for each experiment can be found in Table 4.

Table 2), were highly resistant to oxidation during the PF process. These compounds have high-energy C–F bonding (154 kcal mol^{-1}) and several previous studies indicate that $HO^{\cdot}$ radicals are ineffective in their direct degradation [46,47], with reported kinetic constants for the reaction with $HO^{\cdot} < 10^5$ $M^{-1}s^{-1}$ (Table 2). Of the 4 target PFAS, only PFOA showed ~60 % degradation in Exp. #6. This may be related to its longest chain (C8) since the reaction kinetic is expected to increase with increasing carbon chain [48]. Regarding the PFOA decomposition reaction in the PF process, Liu et al. [49] found that this is probably initiated by electron transfer from PFOA to Fe^{3+}, forming Fe^{2+} and an unstable organic carboxylic radical.

3.1.3. PF-like process with $S_2O_8^{2-}$ as an oxidant

Initially, the UVC/$S_2O_8^{2-}$ process was tested in the absence of the iron catalyst (Exp. #7: UVC + 0.3 mM $S_2O_8^{2-}$). Compared with the results of the UVC/H_2O_2 process (Exp. #1), an increment in the oxidation capacity of CECs was observed (Fig. 4) with removals ranging from 20 % to 40 % for ACK, CBZ-EPX and LSTN, from 40 % to 60 % for ATNL, BSPL, DEET and ISTN, and between 60 % and 80 % for DCF and hormones (E2 and EE2). The improved performance in CECs oxidation obtained for the UVC/$S_2O_8^{2-}$ system can be associated with the advantages of $SO_4^{\cdot-}$ over $HO^{\cdot}$ radicals, such as (i) higher redox potential at neutral pH (2.5–3.1 V *vs* 1.8–2.7 V) and quantum yield, (ii) longer half-life time (30–40 μs *vs* 20 ns), and (iii) enhanced selectivity and high reactivity via electron transfer to organic compounds containing unsaturated or aromatic bonds [50,51]. Furthermore, according to Eqs. (4) and (5) [52], it is possible the occurrence of both $SO_4^{\cdot-}$ and $HO^{\cdot}$ radicals contributing to complementary oxidation pathways for the degradation of the target CECs [53].

$$S_2O_8^{2-} + h\nu \rightarrow 2SO_4^{\cdot-} \ (\lambda = 254\ nm,\ \varepsilon = 21.1\ M^{-1}cm^{-1},\ \varphi = 0.70\ mol\ Einstein^{-1}) \quad (4)$$

$$SO_4^{\cdot-} + H_2O \rightarrow SO_4^{2-} + HO^{\cdot} + H^+ \ (pH\ 5.5-7.0) \quad (5)$$

The addition of the iron catalyst (Exp. #8 and #9) further promotes the generation of $SO_4^{\cdot-}$ and $HO^{\cdot}$ radicals (Eqs. (3) and (6)) and very promising results were registered with ≥ 80 % removal for 13 of the 19 target CECs (Fig. 4). Also noteworthy is the removal of 25 % and 57 % of PFOA (the only PFAS degraded in some extent) and, for the first time, 47

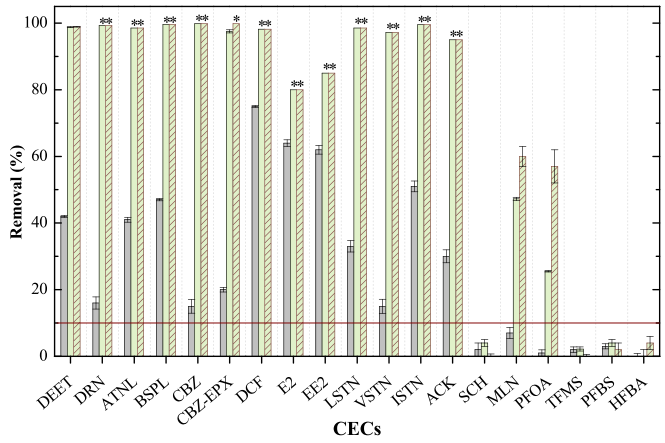

Fig. 4. Removal efficiencies (%) for the 19 target CECs spiked in DW for ( ) Exp. #7, ( ) Exp. #8, and ( ) Exp. #9. *Limit of quantification (see Table 2). The operational conditions for each experiment can be found in Table 4.

% and 60 % of MLN, in Exp. #8 and #9, respectively. However, the 3 remaining PFAS, as well as SCH, were still resistant to the oxidation process. For the same 19 target CECs spiked in DW, by applying an analogous reaction system where the membrane acted as an ozone contactor, very promising degradation results were also obtained using an ozone dose of 12 mg L^{-1} and a RT of 3.9 s [45]. In this case, removals $\geq$ 80 % were also reached for 13 CECs but the 4 PFAS and MLN showed no signs of oxidation. Beyond the recalcitrant nature of PFAS discussed above, this suggests that the generation of $SO_4^{\cdot-}$ is required to oxidize MLN. This agrees with the findings of Maurino et al. [32] who compared different AOPs such as Fenton, sonocatalysis, H_2O_2/UV, and $S_2O_8^{2-}$/UV, and concluded that MLN is able to be degraded by $SO_4^{\cdot-}$ radicals but not by $HO^{\cdot}$ radicals.

$$Fe^{2+} + S_2O_8^{2-} \rightarrow Fe^{3+} + SO_4^{2-} + SO_4^{\cdot-} \quad (6)$$

Greater efficiency of the PF-like process was observed when compared with the PF process under analogous conditions (e.g., Exp. #3 *vs* #8) and even when compared with the traditional PF process performed at a pH of 3.1 (Exp. #6). The superior performance of the PF-like process can be justified not only by the complementary action of $SO_4^{\cdot-}$ and $HO^{\cdot}$ radicals in the oxidation of the target CECs, but also by the more acidic pH (pH_{final} = 4.0 in Exp. #8 and #9 *vs* pH_{final} = 5.5 or 5.6 in Exp. #3 and #4, Table 4), contributing to the maintenance of iron species in the dissolved form and, therefore, to greater production of radical species. The more acidic pH value in the PF-like reaction is related to the lower pH of the $S_2O_8^{2-}$ stock solution compared with the H_2O_2 stock solution (4.1 *vs* 5.4) and the production of H^+ as described in Eq. (5).

3.2. Performance of the PF and PF-like processes in CECs removal using urban wastewater

3.2.1. Effect of residence time and UWW matrix

Due to matrix effects, higher amounts of oxidant ($[H_2O_2]_{ARZ}$ = $[S_2O_8^{2-}]_{ARZ}$ = 1.2 mM) and catalyst ($[Fe^{2+}]_{ARZ}$ = 5 mg L^{-1}) were used in the experiments with UWW, as reported in a previous work [21]. Furthermore, partial recirculation of the effluent was tested by applying different feed-to-recirculation ratios (Q_F/Q_R) in order to increase the RT by 6- and 12-fold (from 6.1 to 36.6 s and 72.3 s) and, consequently, the UVC dose (from 0.1 to 0.6 and 1.2 kJ_{UVC}/L). As RT increased, a clear improvement in the phototreatment performance was observed for both PF and PF-like processes (Fig. 5). This trend is expected and agrees with other studies on CECs degradation in real effluents by PF processes operated in continuous or batch mode, either at optimum or near-neutral pH conditions [14,54].

Despite the difference in performance was not as expressive as that obtained with DW, once again the PF-like process obtained more promising results (Fig. 5a-b). While the PF process had degradations > 60 % for 7 CECs (ACK, CBZ-EPX, DCF, DRN, E2, EE2, and LSTN, Fig. 5a), the PF-like treatment attained oxidation > 60 % for 10 CECs (ACK, ATNL, BSPL, CBZ, CBZ-EPX, DCF, DRN, E2, EE2, and LSTN, Fig. 5b). For the experiments with RT of 6.1 and 36.6 s, it should be noted that the PF-like process (Exp. #16 and #17) recorded higher residual [Fe^{2+}] and [TDI] and, simultaneously, lower precipitation of PO_4^{3-} (Table 4 and Fig. 5c-d) when compared with the PF treatments (Exp. #10 and #11). This feature was also perceived at the end of the treatments by the yellowish coloration of the membrane surface, indicative of the formation of iron precipitates after the PF process (Fig. 5a), and the absence of coloration after the PF-like experiments (Fig. 5b). These are clear indicators that the application of $S_2O_8^{2-}$ brings advantages over H_2O_2 in performing phototreatment under near-neutral pH conditions, as it seems to help to keep the iron species dissolved and avoid their precipitation with PO_4^{3-} (via formation of insoluble iron phosphate salts). Furthermore, with continuous use of this system, it can be anticipated that with the PF-like process, the frequency of necessary cleaning procedures will be much lower than with the PF process. As reported above, the formation of H^+ in the PF-like process (Eq. (5)), and the lower pH of the stock solution of $S_2O_8^{2-}$ when compared with the stock solution of H_2O_2 ($pH\ S_2O_{8stock}^{2-}$ = 4.1 and 5.7 *vs* $pH\ H_2O_{2stock}$ = 5.4 and 6.0, for RT of 6.1 and 36.6 s, respectively) can explain this trend and, therefore, the higher efficiency of the PF-like reaction. Notwithstanding, unlike DW, the pH of UWW at the end of the PF-like treatments remained around 7.5 (Table 4), which is due to the inherent buffering capacity (alkalinity) given by the inorganic carbon content of the UWW (Table 3). With respect to the dissolved inorganic carbon (data in Table SM-2), there was no decrease for both processes when an RT of 6.1 s was applied (Exp. #10 and #16), but it dropped by 10.8 % and 14.8 % for PF and by 13.6 % and 15.7 % for PF-like when using an RT of 36.6 s and 73.2 s, respectively. Regarding mineralization (Table SM-2), no substantial differences were found between RT of 6.1 s and 36.6 s, with the PF experiments registering only ~5 %, and PF-like ~12 %, indicating once again the superior performance of the latter. In turn, for the highest RT tested, mineralization increased to 10 % for PF and 16 % for PF-like, although in these experiments (Exp. #12 *vs* #18), the differences between both processes in relation to the precipitation of iron and PO_4^{3-} were not so obvious (Fig. 5c-d).

Not only the presence of PO_4^{3-} but also a wide variety of inorganic ions (mainly Cl^-, HCO_3^- and CO_3^{2-}) and natural organic matter (NOM) in UWW matrices have been reported to promote an inhibitory effect on CECs degradation kinetics and hence, for decreasing the efficiency of the PF process [20,55]. Different mechanisms can interfere with the degradation of organic compounds, such as the formation of less reactive iron complexes, the reaction of inorganic ions with radicals or the precipitation of iron ions. Additionally, the presence of NOM can compete with the target compounds by interacting with $HO^{\cdot}$ ($k_{HO^{\cdot}, NOM} = 2.23 \times 10^8$ M^{-1} s^{-1} or 1.9×10^4 (mg C L^{-1})$^{-1}$ s^{-1} [56] and, to a lesser extent with $SO_4^{\cdot-}$ ($k_{SO_4^{\cdot-}, NOM} = 6 \times 10^6$ M^{-1} s^{-1} or 5.0×10^2 (mg C L^{-1})$^{-1}$ s^{-1} [57], influencing the degradation of the target pollutants. Conversely, components present in UWW matrices can also promote the PF process by different mechanisms, such as (i) the presence of iron species that can act as an additional source of catalyst, (ii) reaction between Fe^{3+} with other compounds containing –COOH and OH groups, forming complexes with a higher quantum yield, and (iii) the presence of phenolic compounds (inherent reductants) that can promote the reduction of Fe^{3+} to Fe^{2+}, increasing the regeneration rate of the catalyst [55].

3.2.2. Effect of PO_4^{3-} content in UWW

As previously discussed, the complexity of the UWW matrix affects the efficiency of the oxidation processes. Specifically, the presence of PO_4^{3-} in UWW is known to be a strong promoter of iron precipitation

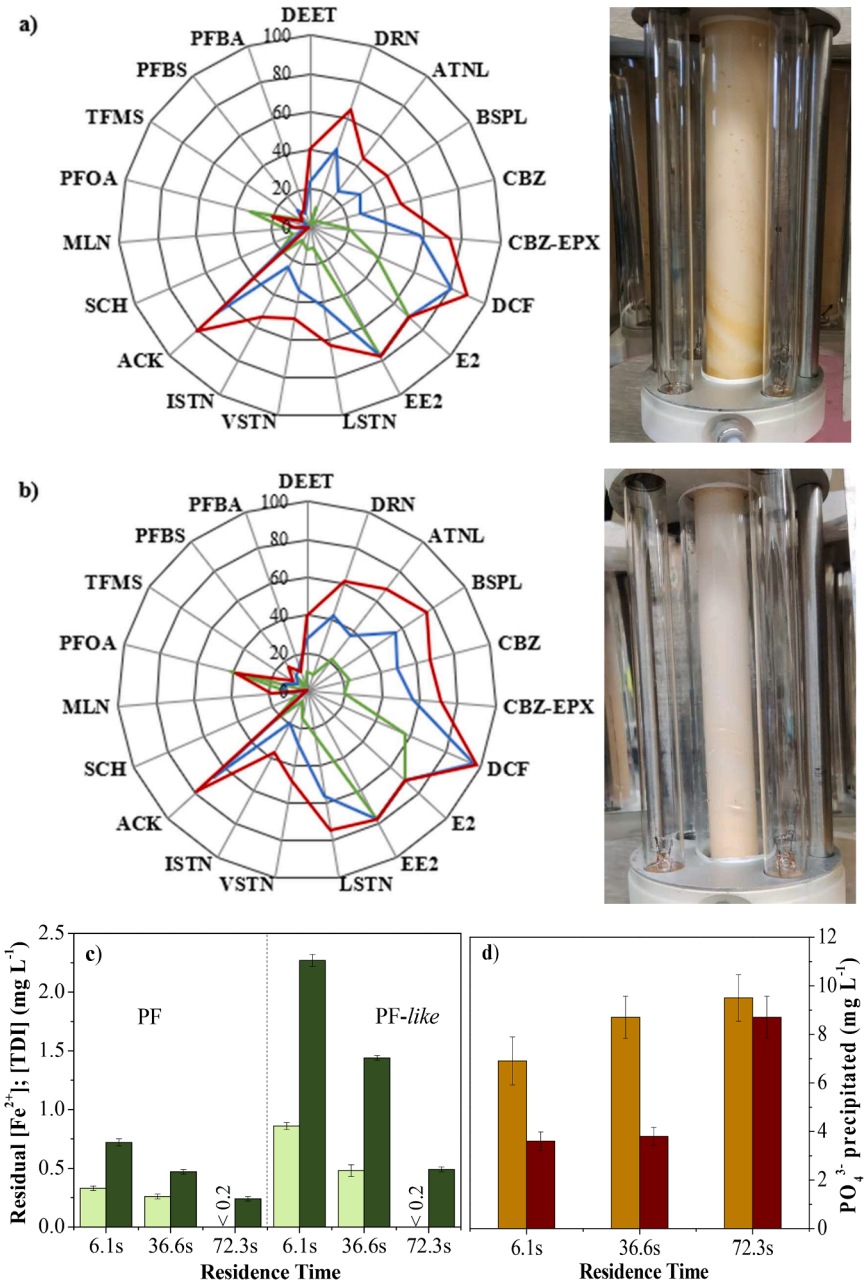

Fig. 5. Removal efficiencies (%) for the 19 target CECs spiked in UWW under different residence times (6.1 s, 36.6 s, and 72.3 s) for the a) PF process (Exp. #10 to #12) and b) PF-like process (Exp. #16 to #18). Photographs of the membrane at the end of the a) PF process Exp. #10 and b) PF-like process Exp. #16. c) Concentration of ( ) residual Fe^{2+} and ( ) total dissolved iron at the end of the experiments under different residence times, and d) PO_4^{3-} precipitated for the ( ) PF and ( ) PF-like process under different residence times. The operational conditions for each experiment can be found in Table 4.

through the formation of strengite, $FePO_4{\cdot}2H_2O$ (s), which not only affects the iron catalyst availability but also light penetration thus impairing the photocatalytic process [20,21]. In this context, additional experiments with previous precipitation (approximately 50 % and 100 %) of PO_4^{3-} present in the UWW (Table 3) were made to assess the effect on CECs removal efficiency. Aluminum sulfate, aluminum oxide, calcium carbonate, lime, and iron salts are found to be quite effective in precipitating phosphates from UWW [58]. Ferrous sulfate salt, which was used as the source of Fe^{2+} in the present work, is also considered a suitable alternative to promote PO_4^{3-} precipitation (Eq. (7) [59].

$$3FeSO_4\cdot + 2PO_4^{3-} \rightarrow Fe_3(PO_4)2 + 3SO_4^{2-} \quad (7)$$

When compared with the experiments without previous PO_4^{3-} precipitation under the same operating conditions (Exp.#12 *vs* #13 and #14 and Exp.#18 *vs* #19 and #20), for both PF and PF-like processes a reduction in the performance for CECs removal was observed (Fig. 6). This can be related to the increase in TSS concentration, from 4 to 44.3 and 67.7 mg L^{-1} for the experiments without and with ~50 % and ~100 % PO_4^{3-} precipitation, respectively (Table 3). The presence of small precipitated aggregates decreases light penetration into the reaction medium (scattering effects) [60], decreasing the direct photolysis of CECs, oxidants, and ferric species. Consequently, process efficiency was also tested on the effluent with ~100 % PO_4^{3-} precipitation followed by filtration (Exp. #15 for PF, and Exp. #21, for PF-like, Table 4) and a clear improvement in CECs removal was obtained (Fig. 6). However, when compared with the experiments without prior PO_4^{3-} precipitation (Exp. #12 *vs* #15 and Exp.#18 *vs* #21), only slight differences in the CECs removal efficiency were observed (Fig. 6). Similar trend was also

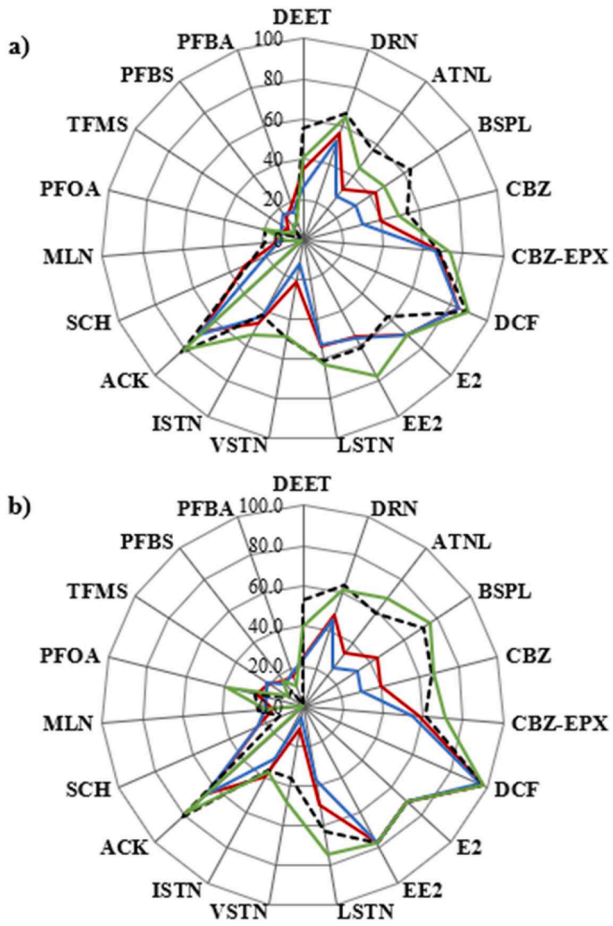

Fig. 6. Removal efficiencies (%) of 19 target CECs spiked in UWW for the a) PF process (Exp. #12 to #15) and b) PF-like process (Exp. #18 to #21): (—) without PO_4^{3-} precipitation; (—) with 50% PO_4^{3-} precipitation; (—) with 100% PO_4^{3-} precipitation; and (— —) with 100% PO_4^{3-} precipitation and post-filtration. The operational conditions for each experiment can be found in Table 4.

verified regarding the removal of organic carbon (2.4 mg C L^{-1}, for both Exp. #12 and #15, and 3.9 and 3.7 mg C L^{-1}, for Exp. #18 and #21, respectively, data available in Table SM-2). Considering that the UWW used in the tests had a similar composition in TSS (4.0 *vs* 6.3 mg L^{-1}, Table 3), but presented a large difference in the concentration of PO_4^{3-} (16.8 *vs* 0.97 mg L^{-1}, Table 3), these results suggest that the influence of the initial concentration of PO_4^{3-} in the UWW had a minor or negligible impact over the overall efficiency for both processes. This feature can be related to the advantages offered by the radial addition of the iron catalyst in the tubular membrane reactor. The continuous "titration" of small iron dosages along the reactor length is expected to minimize the deleterious effects of iron precipitates when compared to systems where the catalyst is delivered at the inlet of the reactor. This was perceived in the work of De la Cruz et al. [61], where the iron was added at the inlet of a cylindrical reactor (37 L capacity enclosing static mixers and five low-pressure mercury UVC lamps of 150 W each) to test PF treatment at near-neutral pH conditions for the removal of 22 CECs naturally present in secondary-treated UWW. The authors reported that iron precipitation negatively affected the phototreatment efficiency and lower degradation rates were observed when compared with the UV_{254}/H_2O_2 process (62 % drop when applying 4 mg Fe^{3+} L^{-1}).

PO_4^{3-} is an essential nutrient for plant growth, but at the same time, it is limited and concentrated in some countries outside Europe and its recovery becomes necessary. Furthermore, it has been suggested the importance of including metals, especially iron, in phosphate recovery [62]. Therefore, its precipitation before or after the PF oxidation system, makes it possible to recover this essential nutrient and contribute to a circular economy perspective.

4. Conclusions

A tubular membrane photoreactor, operated in continuous mode with low residence times and applying a smart dose strategy for Fe^{2+}, was used to promote the PF ($UVC/Fe^{2+}/H_2O_2$) and PF-like ($UVC/Fe^{2+}/S_2O_8^{2-}$) processes under near-neutral pH conditions for the oxidation of 19 CECs in the tertiary treatment of UWW. Although certain short-chain PFAS and the artificial sweetener saccharine exhibited their recalcitrant character to all conditions tested, the PF-like process demonstrated superior oxidation capacity when compared with the PF process, achieving higher removals for most target contaminants, particularly for melamine. The activation of $S_2O_8^{2-}$ not only induces pH decay, contributing to the permanence of dissolved iron species as verified by the lower precipitation of phosphate, but is also able of generating both $SO_4^{\cdot-}$ and $HO^{\cdot}$ radicals that can act in complementary oxidation pathways boosting CECs degradation.

Overall, our results highlight the importance of photoreactor design to achieve efficient PF processes at neutral pH without supplying additional chemical agents. The unique configuration of the tubular membrane photoreactor allows a homogeneous axial and radial distribution of the acidic Fe^{2+} stock solution, fed through the membrane pores, enabling a more efficient conversion of Fe^{3+} to Fe^{2+} in contact with UVC light, minimizing the precipitation of iron to some extent and enhancing the formation of oxidative radicals. Moreover, the continuous "titration" of small catalyst doses permits a low final iron concentration, which is important for meeting discharge limits or water reuse purposes. In addition to the removal of micropollutants, the simultaneous removal of PO_4^{3-} through the formation of strengite appears as a further advantage, being fundamental in the introduction of reuse, recycling and resource recovery paradigms in wastewater management. Nonetheless, our findings emphasize the need for further research to address the challenges associated with recalcitrant CECs and the potential formation of transformation products to ensure the safety of the treatment approach.

Declaration of Competing Interest

The authors declare that they have no known competing financial interests or personal relationships that could have appeared to influence the work reported in this paper.

Data availability

No data was used for the research described in the article.

Acknowledgements

The financial support for this work results from: (i) Project NORWATER funded by INTERREG VA Spain-Portugal cooperation programme, Cross-Border North Portugal/Galizia Spain Cooperation Programme (POCTEP), ref. 0725_NOR_WATER_1_P; (ii) Project "Healthy Waters – Identification, Elimination, Social Awareness and Education of Water Chemical and Biological Micropollutants with Health and Environmental Implications", with reference NORTE-01-0145-FEDER-000069, supported by Norte Portugal Regional Operational Programme (NORTE 2020), under the PORTUGAL 2020 Partnership Agreement, through the European Regional Development Fund (ERDF), (iii) LA/P/0045/2020 (ALiCE), UIDB/50020/2020 and UIDP/50020/2020 (LSRE-LCM), funded by national funds through FCT/MCTES (PIDDAC). The authors would like to thank the EU and Bundesministerium für Bildung und Forschung, Germany, Ministero dell'Università e della Ricerca, Italy, Agencia Estatal de Investigación - MCIN/AEI/10.13039/501100011033 (ref. PID2020-117686RB-C32) and Xunta de

Galicia (ED431C 2021/06), Spain, Fundação para a Ciência e a Tecnologia, Portugal, Norges forskningsråd, Norway, Water Research Commission, South Africa for funding, in the frame of the collaborative international consortium SERPIC financed under the ERA-NET AquaticPollutants Joint Transnational Call (GA N° 869178).

Appendix A. Supplementary data

Supplementary data to this article can be found online at https://doi.org/10.1016/j.cej.2023.146655.

References

[1] M.O. Barbosa, N.F.F. Moreira, A.R. Ribeiro, M.F.R. Pereira, A.M.T. Silva, Occurrence and removal of organic micropollutants: An overview of the watch list of EU Decision 2015/495, Water Res. 94 (2016) 257–279, https://doi.org/10.1016/j.watres.2016.02.047.

[2] P. Krzeminski, M.C. Tomei, P. Karaolia, A. Langenhoff, C.M.R. Almeida, E. Felis, F. Gritten, H.R. Andersen, T. Fernandes, C.M. Manaia, L. Rizzo, D. Fatta-Kassinos, Performance of secondary wastewater treatment methods for the removal of contaminants of emerging concern implicated in crop uptake and antibiotic resistance spread: A review, Sci. Total Environ. 648 (2019) 1052–1081, https://doi.org/10.1016/j.scitotenv.2018.08.130.

[3] I.Y. López-Pacheco, A. Silva-Núñez, C. Salinas-Salazar, A. Arévalo-Gallegos, L. A. Lizarazo-Holguin, D. Barceló, H.M.N. Iqbal, R. Parra-Saldívar, Anthropogenic contaminants of high concern: Existence in water resources and their adverse effects, Sci. Total Environ. 690 (2019) 1068–1088, https://doi.org/10.1016/j.scitotenv.2019.07.052.

[4] V.K. Parida, D. Saidulu, A. Majumder, A. Srivastava, B. Gupta, A.K. Gupta, Emerging contaminants in wastewater: A critical review on occurrence, existing legislations, risk assessment, and sustainable treatment alternatives, J. Environ. Chem. Eng. 9 (5) (2021), 105966, https://doi.org/10.1016/j.jece.2021.105966.

[5] E. Gualda-Alonso, P. Soriano-Molina, J.L. Casa López, J.L. García Sánchez, P. Plaza-Bolaños, A. Agüera, J.A. Sánchez Pérez, Large-scale raceway pond reactor for CEC removal from municipal WWTP effluents by solar photo-Fenton, Appl Catal B 319 (2022), 121908, https://doi.org/10.1016/j.apcatb.2022.121908.

[6] I. Oller, S. Malato, Photo-Fenton applied to the removal of pharmaceutical and other pollutants of emerging concern, Curr. Opin. Green Sustainable Chem. 29 (2021), 100458, https://doi.org/10.1016/j.cogsc.2021.100458.

[7] S. Rodriguez, L. Vasquez, D. Costa, A. Romero, A. Santos, Oxidation of Orange G by persulfate activated by Fe(II), Fe(III) and zero valent iron (ZVI), Chemosphere 101 (2014) 86–92, https://doi.org/10.1016/j.chemosphere.2013.12.037.

[8] Y. Wu, R. Prulho, M. Brigante, W. Dong, K. Hanna, G. Mailhot, Activation of persulfate by Fe(III) species: Implications for 4-tert-butylphenol degradation, J. Hazard. Mater. 322 (2017) 380–386, https://doi.org/10.1016/j.jhazmat.2016.10.013.

[9] S. Luo, Z. Wei, D.D. Dionysiou, R. Spinney, W.-P. Hu, L. Chai, Z. Yang, T. Ye, R. Xiao, Mechanistic insight into reactivity of sulfate radical with aromatic contaminants through single-electron transfer pathway, Chem. Eng. J. 327 (2017) 1056–1065, https://doi.org/10.1016/j.cej.2017.06.179.

[10] R. Xiao, Z. Luo, Z. Wei, S. Luo, R. Spinney, W. Yang, D.D. Dionysiou, Activation of peroxymonosulfate/persulfate by nanomaterials for sulfate radical-based advanced oxidation technologies, Curr. Opin. Chem. Eng. 19 (2018) 51–58, https://doi.org/10.1016/j.coche.2017.12.005.

[11] J.J. Pignatello, E. Oliveros, A. Mackay, Advanced Oxidation Processes for Organic Contaminant Destruction Based on the Fenton Reaction and Related Chemistry, Crit. Rev. Environ. Sci. Technol. 36 (1) (2007) 1–84, https://doi.org/10.1080/10643380500326564.

[12] N. López-Vinent, A. Cruz-Alcade, J.A. Malvestiti, P. Marco, J. Giménez, S. Esplugas, Organic fertilizer as a chelating agent in photo-Fenton at neutral pH with LEDs for agricultural wastewater reuse: Micropollutant abatement and bacterial inactivation, Chem. Eng. J. 388 (2020), 124246, https://doi.org/10.1016/j.cej.2020.124246.

[13] S. Arzate, M.C. Campos-Mañas, S. Miralles-Cuevas, A. Agüera, J.L. García Sánchez, J.A. Sánchez Pérez, Removal of contaminants of emerging concern by continuous flow solar photo-Fenton process at neutral pH in open reactors, J. Environ. Manage. 261 (2020), 110265, https://doi.org/10.1016/j.jenvman.2020.110265.

[14] N. Klemerth, S. Malato, A. Agüera, A. Fernández-Alba, Photo-Fenton and modified photo-Fenton at neutral pH for the treatment of emerging contaminants in wastewater treatment plant effluents: A comparison, Water Res. 47 (2) (2013) 833–840, https://doi.org/10.1016/j.watres.2012.11.008.

[15] I. Carra, J.L.C. López, L. Santos-Juanes, S. Malato, J.A. Sánchez Pérez, Iron dosage as a strategy to operate the photo-Fenton process at initial neutral pH, Chem. Eng. J. 224 (2013) 67–74, https://doi.org/10.1016/j.cej.2012.09.065.

[16] A. Mejri, P. Soriano-Molina, S. Miralles-Cuevas, J.A. Sánchez Pérez, Fe3+-NTA as iron source for solar photo-Fenton at neutral pH in raceway pond reactors, Sci. Total Environ. 736 (2020), 139617, https://doi.org/10.1016/j.scitotenv.2020.139617.

[17] M.C.V.M. Starling, E.P. Costa, F.A. Souza, E.C. Machado, J.C. Araujo, C.C. Amorim, Persulfate mediated solar photo-Fenton aiming at wastewater treatment plant effluent improvement at neutral PH: emerging contaminant removal, disinfection, and elimination of antibiotic-resistant bacteria, Environ. Sci. Pollut. Res. 28 (2021) 17355–17368, https://doi.org/10.1007/s11356-020-11802-z.

[18] W. Dong, Y. Jin, K. Zhou, S.-P. Sun, Y. Li, X.D. Chen, Efficient degradation of pharmaceutical micropollutants in water and wastewater by FeIII-NTA-catalyzed neutral photo-Fenton process, Sci. Total Environ. 688 (2019) 513–520, https://doi.org/10.1016/j.scitotenv.2019.06.315.

[19] P. Soriano-Molina, S. Miralles-Cuevas, B.E. García, P. Plaza-Bolaños, J.A. Sánchez Pérez, Two strategies of solar photo-Fenton at neutral pH for the simultaneous disinfection and removal of contaminants of emerging concern. Comparative assessment in raceway pond reactors, Catal. Today 361 (2021) 17–23, https://doi.org/10.1016/j.cattod.2019.11.028.

[20] A.A. Nogueira, B.M. Souza, M.W.C. Dezotti, R.A.R. Boaventura, V.J.P. Vilar, Ferrioxalate complexes as strategy to drive a photo-FENTON reaction at mild pH conditions: A case study on levofloxacin oxidation, J. Photochemistry Photobiology A: Chem. 345 (2017) 109–123, https://doi.org/10.1016/j.jphotochem.2017.05.020.

[21] J. Díaz-Angulo, S. Cotillas, A.I. Gomes, S.M. Miranda, M. Mueses, F. Machuca-Martínez, M.A. Rodrigo, R.A.R. Boaventura, V.J.P. Vilar, A tube-in-tube membrane microreactor for tertiary treatment of urban wastewaters by photo-Fenton at neutral pH: A proof of concept, Chemosphere 263 (2021), 128049, https://doi.org/10.1016/j.chemosphere.2020.128049.

[22] U.J. Ahile, R.A. Wuana, A.U. Itodo, R. Sha'Ato, R.F. Dantas, A review on the use of chelating agents as an alternative to promote photo-Fenton at neutral pH: Current trends, knowledge gap and future studies, Sci. Total Environ. 710 (2020), 134872, https://doi.org/10.1016/j.scitotenv.2019.134872.

[23] R. Montes, S. Méndez, N. Carro, J. Cobas, N. Alves, T. Neuparth, M.M. Santos, J. B. Quintana, R. Rodil, Screening of Contaminants of Emerging Concern in Surface Water and Wastewater Effluents, Assisted by the Persistency-Mobility-Toxicity Criteria, Molecules 27 (12) (2022) 3915, https://doi.org/10.3390/molecules27123915.

[24] R. Montes, S. Méndez, J. Cobas, N. Carro, T. Neuparth, N. Alves, M.M. Santos, J. B. Quintana, R. Rodil, Occurrence of persistent and mobile chemicals and other contaminants of emerging concern in Spanish and Portuguese wastewater treatment plants, transnational river basins and coastal water, Sci. Total Environ. 885 (2023), 163737, https://doi.org/10.1016/j.scitotenv.2023.163737.

[25] M.M. Ahmed, S. Barbati, P. Doumeng, S. Chiron, Sulfate radical anion oxidation of diclofenac and sulfamethoxazole for water decontamination, Chem. Eng. J. 197 (2012) 440–447, https://doi.org/10.1016/j.cej.2012.05.040.

[26] C. Ye, X. Ma, J. Deng, X. Li, Q. Li, A.M. Dietrich, Degradation of saccharin by UV/H2O2 and UV/PS processes: A comparative study, Chemosphere 288 (2022), 132337, https://doi.org/10.1016/j.chemosphere.2021.132337.

[27] J.E. Toth, K.A. Rickman, A.R. Venter, J.J. Kiddle, S.P. Mezyk, Reaction Kinetics and Efficiencies for the Hydroxyl and Sulfate Radical Based Oxidation of Artificial Sweeteners in Water, Chem. A Eur. J. 116 (40) (2012) 9819–9824, https://doi.org/10.1021/jp3047246.

[28] D. Stauter, A. Dabrowska, R. Bloch, M. Stapf, U. Miehe, A. Sperlich, R. Gnirss, T. Wintgens, Deep-bed filters as post-treatment for ozonation in tertiary municipal wastewater treatment: impact of design and operation on treatment goals, Environ. Sci. Water Res. Technol. 7 (2021) 197–211, https://doi.org/10.1039/D0EW00684J.

[29] K. Zhou, Z. Wang, X. Wang, G. Jiao, Y. Li, S.-P. Sun, X.D. Chen, Degradation of emerging pharmaceutical micropollutants in municipal secondary effluents by low-pressure UVC-activated HSO_5^- and $S_2O_8^{2-}$ AOPs, Chem. Eng. J. 393 (2020), 124712, https://doi.org/10.1016/j.cej.2020.124712.

[30] L. Lian, B. Yao, S. Hou, J. Fang, S. Yan, W. Song, Kinetic Study of Hydroxyl and Sulfate Radical-Mediated Oxidation of Pharmaceuticals in Wastewater Effluents, Environ. Sci. Tech. 51 (5) (2017) 2954–2962, https://doi.org/10.1021/acs.est.6b05536.

[31] W. Song, W.J. Cooper, B.M. Peake, S.P. Mezyk, M.G. Nickelsen, K.E. O'Shea, Free-radical-induced oxidative and reductive degradation of N, N'-diethyl-m-toluamide (DEET): Kinetic studies and degradation pathway, Water Res. 43 (3) (2008) 635–642, https://doi.org/10.1016/j.watres.2008.11.018.

[32] V. Maurino, M. Minella, F. Sordello, C. Minero, A proof of the direct hole transfer in photocatalysis: The case of melamine, Appl. Catal. A 521 (2016) 57–67, https://doi.org/10.1016/j.apcata.2015.11.012.

[33] M. Umar, Reductive and Oxidative UV Degradation of PFAS—Status, Needs and Future Perspectives. Water 13 (22) (2021) 3185, https://doi.org/10.3390/w13223185.

[34] Y. Qian, X. Guo, Y. Zhang, Y. Peng, P. Sun, C.-H. Huang, J. Niu, X. Zhou, J. C. Crittenden, Perfluorooctanoic Acid Degradation Using UV–Persulfate Process: Modeling of the Degradation and Chlorate Formation, Environ. Sci. Tech. 50 (2) (2016) 772–781.

[35] S.P. Mezyk, E.M. Abud, K.L. Swancutt, G. McKay, D.D. Dionysiou, Contaminants of Emerging Concern in the Environment: Ecological and Human Health Considerations. Halden, R.U. (ed), American Chemical Society, 2010.

[36] M. Bourgin, B. Beck, M. Boehler, E. Borowska, J. Fleiner, E. Salhi, R. Teichler, U. von Guten, H. Siegrist, C.S. McArdell, Evaluation of a full-scale wastewater treatment plant upgraded with ozonation and biological post-treatments: Abatement of micropollutants, formation of transformation products and oxidation by-products, Water Res. 129 (2018) 486–498, https://doi.org/10.1016/j.watres.2017.10.036.

[37] M.M. Huber, S. Canonica, G.-Y. Park, U. von Guten, Oxidation of Pharmaceuticals during Ozonation and Advanced Oxidation Processes, Environ. Sci. Tech. 37 (5) (2003) 1016–1024, https://doi.org/10.1021/es025896h.

[38] Y.F. Rao, L. Qu, H. Yang, W. Chu, Degradation of carbamazepine by Fe(II)-activated persulfate process, J. Hazard. Mater. 268 (2014) 23–32, https://doi.org/10.1016/j.jhazmat.2014.01.010.
[39] V.J.P. Vilar, P. Alfonso-Muniozguren, J.P. Monteiro, J. Lee, S.M. Miranda, R.A. R. Boaventura, Tube-in-tube membrane microreactor for photochemical UVC/H2O2 processes: A proof of concept, Chem. Eng. J. 379 (2020), 122341, https://doi.org/10.1016/j.cej.2019.122341.
[40] C.G. Hatchard, C.A. Parker, A new sensitive chemical actinometer. II. Potassium ferrioxalate as a standard chemical actinometer, Proc. R. Soc. A 235 (1956) 518–536, https://doi.org/10.1098/rspa.1956.0102.
[41] R.S. Ayers, D.W. Westcot, (1985, rev. 1994) Water quality for agriculture: guidelines, Food and Agriculture Organization of the United Nations, Rome.
[42] R.F.P. Nogueira, M.C. Oliveira, W.C. Paterlini, Simple and fast spectrophotometric determination of H_2O_2 in photo-Fenton reactions using metavanadate, Talanta 66 (2005) 86–91, https://doi.org/10.1016/j.talanta.2004.10.001.
[43] C. Liang, C.F. Huang, N. Mohanty, R.M. Kurakalva, A rapid spectrophotometric determination of persulfate anion in ISCO, Chemosphere 73 (2008) 1540–1543, https://doi.org/10.1016/j.chemosphere.2008.08.043.
[44] ISO, I.O.f.S. 1988 ISO6332: Water quality — Determination of iron — Spectrometric method using 1,10-phenanthroline.
[45] P.H. Presumido, R. Montes, J.B. Quintana, R. Rodil, M. Feliciano, G.L. Puma, A. I. Gomes, V.J.P. Vilar, Ozone membrane contactor to intensify gas/liquid mass transfer and contaminants of emerging concern oxidation, J. Environ. Chem. Eng. 10 (6) (2022), 108671, https://doi.org/10.1016/j.jece.2022.108671.
[46] H.F. Schröder, R.J.W. Meesters, Stability of fluorinated surfactants in advanced oxidation processes—A follow up of degradation products using flow injection–mass spectrometry, liquid chromatography–mass spectrometry and liquid chromatography–multiple stage mass spectrometry, J. Chromatogr. A 1082 (1) (2005) 110–119, https://doi.org/10.1016/j.chroma.2005.02.070.
[47] M. Trojanowicz, A. Bojanowska-Czajka, I. Bartosiewicz, K. Kulisa, Advanced Oxidation/Reduction Processes treatment for aqueous perfluorooctanoate (PFOA) and perfluorooctanesulfonate (PFOS) – A review of recent advances, Chem. Eng. J. 336 (2018) 170–199, https://doi.org/10.1016/j.cej.2017.10.153.
[48] Q. Zhuo, S. Deng, B. Yang, J. Huang, B. Wang, T. Zhang, G. Yu, Degradation of perfluorinated compounds on a boron-doped diamond electrode, Electrochim. Acta 77 (2012) 17–22, https://doi.org/10.1016/j.electacta.2012.04.145.
[49] D. Liu, Z. Xiu, F. Liu, G. Wu, D. Adamson, C. Newell, P. Vikesland, A.-L. Tsai, P. J. Alvarez, Perfluorooctanoic acid degradation in the presence of Fe(III) under natural sunlight, J. Hazard. Mater. 262 (2013) 456–463, https://doi.org/10.1016/j.jhazmat.2013.09.001.
[50] S. Giannakis, K.-Y.-A. Lin, F. Ghanbari, A review of the recent advances on the treatment of industrial wastewaters by Sulfate Radical-based Advanced Oxidation Processes (SR-AOPs), Chem. Eng. J. 406 (2021), 127083, https://doi.org/10.1016/j.cej.2020.127083.
[51] S. Guerra-Rodríguez, E. Rodríguez, D.N. Singh, J. Rodríguez-Chueca, Assessment of Sulfate Radical-Based Advanced Oxidation Processes for Water and Wastewater Treatment: A Review, Water 10 (12) (2018) 1828, https://doi.org/10.3390/w10121828.
[52] N.K. Vel Leitner, Advanced Oxidation Processes for Water Treatment: Fundamentals and Applications. Stefan, M.I. (ed), IWA Publishing, London, UK, 2018.
[53] L. Vazquez, L.M.M.T. Gomes, P.H. Presumido, D.G.D. Rocca, R.F.P.M. Moreira, T. Dagnac, M. Llompart, A.I. Gomes, V.J.P. Vilar, Tubular membrane photoreactor for the tertiary treatment of urban wastewater towards antibiotics removal: application of different photocatalyst/oxidant combinations and ozonation, J. Environ. Chem. Eng. 11 (3) (2023), 109766, https://doi.org/10.1016/j.jece.2023.109766.
[54] S. Arzate, J.L. García Sánchez, P. Soriano-Molina, J.L. Casa López, M.C. Campos-Mañas, A. Agüera, J.A. Sánchez Pérez, Effect of residence time on micropollutant removal in WWTP secondary effluents by continuous solar photo-Fenton process in raceway pond reactors, Chem. Eng. J. 316 (2017) 1114–1121, https://doi.org/10.1016/j.cej.2017.01.089.
[55] A.R. Ribeiro, N.F.F. Moreira, G. Li Puma, A.M.T. Silva, Impact of water matrix on the removal of micropollutants by advanced oxidation technologies, Chem. Eng. J. 363 (2019) 155–173, https://doi.org/10.1016/j.cej.2019.01.080.
[56] P. Westerhoff, S.P. Mezyk, J. Cooper, D. Minakata, Electron Pulse Radiolysis Determination of Hydroxyl Radical Rate Constants with Suwannee River Fulvic Acid and Other Dissolved Organic Matter Isolates, Environ. Sci. Tech. 41 (13) (2007) 4640–4646, https://doi.org/10.1021/es062529n.
[57] A. Behnami, E. Aghayani, K.Z. Benis, M. Sattari, M. Pourakbar, Comparing the efficacy of various methods for sulfate radical generation for antibiotics degradation in synthetic wastewater: degradation mechanism, kinetics study, and toxicity assessment, RSC Adv. 12 (2022) 14945–14956, https://doi.org/10.1039/D2RA01618D.
[58] M.L. Christensen, C. Cvitanich, C.A. Quist-Jensen, M. Thau, B. Malmgren-Hansen, Precipitation and recovery of phosphorus from the wastewater hydrolysis tank, Sci. Total Environ. 813 (2022), 151875, https://doi.org/10.1016/j.scitotenv.2021.151875.
[59] G. Badea, M.-D. Roman, I. Giurca, C.O. Safirescu, I. Aschilean, D. Muresan, Chemical precipitation of phosphorus on a wastewater treatment pilot plant Lee, K. C. (ed), Budapeste, Hungary, 2013.
[60] A.I. Gomes, S.G.S. Santos, T.F.C.V. Silva, R.A.R. Boaventura, V.J.P. Vilar, Treatment train for mature landfill leachates: Optimization studies, Sci. Total Environ. 673 (2019) 470–479, https://doi.org/10.1016/j.scitotenv.2019.04.027.
[61] N. De la Cruz, L. Esquius, D. Grandjean, A. Magnet, A. Tungler, L.F. Alencastro, C. Pulgarín, Degradation of emergent contaminants by UV, UV/H2O2 and neutral photo-Fenton at pilot scale in a domestic wastewater treatment plant, Water Res. 47 (15) (2013) 5836–5845, https://doi.org/10.1016/j.watres.2013.07.005.
[62] V. Bohra, K.U. Ahamad, A. Kela, G. Vaghela, A. Sharma, B.J. Deka, Clean Energy and Resource Recovery (2022) 17–36.